

Dedicated to Prof. Dorin N. Poenaru's
70th Anniversary

STABILITY OF CHARGED ATOMIC CLUSTERS

A.G. LYALIN¹, O.I. OBOLENSKY^{1,2}, A.V. SOLOV'YOV^{1,2}, W. GREINER¹

¹Frankfurt Institute for Advanced Studies, J.W. Goethe University
Max-von-Laue-Str. 1, D-60438 Frankfurt am Main, Germany
E-mail: solovyov@fias.uni-frankfurt.de

²On leave from A.F. Ioffe Physical-Technical Institute, 194021 St. Petersburg, Russia

(Received February 21, 2007)

Abstract. Advances achieved during recent years in model and *ab initio* descriptions of fission of atomic clusters are reviewed. We focus on developments in *ab initio* treatment of the electronic subsystem within the jellium background model, as well as on applications of potential energy surface analysis to determining the characteristics of the fission process. We reiterate the main results obtained with the implementation of the Hartree-Fock and local density schemes for the two-center deformed jellium model.

Key words: atomic clusters, fission reactions, stability.

1. INTRODUCTION

Stability of atomic clusters is an ubiquitous phenomenon that is encountered in various branches of science, from nuclear, atomic, molecular and solid state physics, to chemistry and biology. In this paper we will restrict ourselves to study stability and fragmentation of charged atomic clusters.

The process of fragmentation of a charged cluster in which at least two of the daughter fragments are charged is called fission. Previous reviews of theoretical methods and the experimental techniques and results devoted to fission of charged atomic clusters can be found in Refs. [1–5].

Theory of cluster fission is a very interesting and important subject, not only because it has immediate applications in experiment and nanotechnology but also because cluster fission presents one of the instances of a long standing fundamental problem of stability of complex systems. A detailed description of different aspects of this process requires an interdisciplinary approach combining methods of atomic, molecular and nuclear physics, thermodynamics,

statistics, mathematics and computational science. Fission of charged metal clusters provides especially close analogies to the corresponding process in nuclear systems. Many approaches used for treatment of fission of charged metal clusters are borrowed from the theory of nuclear fission [1]. On the other hand, methods which proved to be effective and reliable for description of fission of metal clusters can be readily applied for analysis of the fission phenomenon in other complex systems, e.g., in biomolecules [6,7].

Coulomb repulsion is the driving force of the fission process. Depending on the excessive charge and cluster size, charged clusters can be found in the stable, metastable or unstable states. In the unstable states the Coulomb repulsion is so strong that the cluster immediately decays into two or more fragments (the so-called Coulomb explosion). The Coulomb explosion is typical for high ratios of excessive charge to cluster size.

At lower degrees of the cluster ionization an interplay between the electronic binding and the Coulomb repulsion results in formation of a potential barrier which prevents the cluster from immediate decay [1,8–14]. Since the tunneling is a negligible effect for clusters due to their large masses and large barrier widths (in contrast to nuclear fission), overcoming the fission barrier requires additional energy¹ to be transferred to the cluster, even though the energy of the system in the final state can be lower than the energy of the initial (unfragmented) state. The minimum amount of energy, which has to be transferred to the cluster in order for fission to become possible, equals to the height of the fission barrier. Therefore, this quantity plays a crucial role in defining the characteristics of the fission process.

Large clusters with relatively small excessive charges are intrinsically stable since the energy of the parent cluster is lower than the sum of the energies of the daughter fragments and fission is a purely endothermic reaction. The leading fragmentation mechanism in this case is evaporation of small neutral fragments which in most cases has smaller activation energy than fission.²

Usually only stable clusters are observed in experiments, whose sizes exceed the so called “appearance size”,³ the size at which the evaporation rate becomes smaller or equal to the rate of fission or, similarly, the size at which the fission barrier becomes lower than the evaporation energy [11]. In a typical experimental set up, an ensemble of clusters of different sizes is created. Larger clusters gradually decrease their size by evaporating neutral monomers or dimers until they reach the “appearance size” at which fission becomes the dominant process. This results in abrupt disappearance of smaller clusters

¹ For Coulomb explosion the height of the barrier is zero. In this case fission is a barrierless process.

² Usually, one distinguishes between fission, driven by Coulomb repulsive forces, and evaporation of neutral fragments (normally, only monomers and dimers are evaporated).

³ Also called sometimes “critical size”.

(of the same excessive charge) from the experimental mass spectra, since such clusters fission into less charged fragments before they are detected. The “appearance size” depends on the metal species and cluster charge [9, 10, 15–19]. Other experimental set ups are possible which allow one to investigate properties of clusters of preselected size and charge, see, e.g. Ref. [20] and references therein.

Approaches used for describing the fission process and determining the height and shape of the fission barrier can be divided into two large groups. The first group is characterized by averaging over the positions of the atomic ions within a fixed cluster volume. The point Coulomb charges of the ions are replaced by a uniform positively charged background jellium. Such replacement is quite natural since the electrons in metal clusters are delocalized and details of ionic structure are not essential in treatment of the electronic subsystem. The approximation of the jellium background allows one to reveal the underlying physics of most of the phenomena inherent to the fission process and to obtain reasonable agreement with experiment [1, 21]. In the second group of approaches the positions of the atomic ions are retained as independent variables see, e.g. [5, 22–31] and references therein. This substantially complicates the calculations but allows one to study the effects which are beyond the scope of the jellium model, for example, an influence of cluster geometry on thermodynamical characteristics of the fission process [22]. Explicit account for positions of the nuclei in the cluster also removes the problem of parametrization of the shape of the jellium. The height and the shape of the fission barrier are very sensitive to an inevitable arbitrariness in parametrization of the shape of the cluster in the vicinity of the scission point (which usually corresponds to the top of the barrier).

Perhaps, the simplest model among the background jellium models is the Liquid Drop Model (LDM), which is based on investigations of instabilities in charged droplets carried out by Lord Rayleigh in 1882 [32]. This model was later widely used in nuclear physics, and subsequently adapted to charged metal clusters [33, 34]. In this model, one introduces the “fissility parameter”, $X = E_{Coul}^{sphere} / 2E_{Surf}^{sphere}$, which is proportional to the ratio of the Coulomb to surface energy of charged spherical liquid drop [32]. The fissility parameter distinguishes the situations when cluster is unstable, metastable, or stable. The investigation of the Rayleigh instabilities in multiply charged sodium clusters has been done in Ref. [35], where reasonable agreement with experimental data was found.

One of the main deficiencies of the LDM is neglecting quantum mechanical shell effects. It has been shown that the shell effects are important in fission of nuclei [36] and metal clusters [19]. One can describe the shell effects in metal clusters using the Shell Correction Method (SCM), originally

developed in nuclear physics [36–38]. This method was adapted for metal clusters in Refs. [39–43]. The asymmetric two-center-oscillator shell model (ATCOSM), introduced in Ref. [44] for nuclear fission is quite successful in prediction of the fission barriers. This model was also applied for the description of metal cluster fission [45]. Even though ATCOSM method uses single electron model potential it has the significant advantage in comparison to other models allowing a simple shape parametrization and an independent variation of deformations in the parent and daughter clusters [45].

Fission process of metal clusters can be also simulated on the basis of the self-consistent many-body *ab initio* schemes for treating the electronic subsystem, such as the density functional theory (DFT) or the Hartree-Fock (HF) approach combined with the jellium model. Within this approach the electrons are considered in the usual quantum mechanical way, while the cluster core potential is approximated by the potential of the homogeneous positively charged background [46]. The important feature of the DFT methods consists in the fact that they account for many-electron correlations, via the phenomenological exchange-correlation potentials (see, e.g., Refs. [47–49] for a review). The Local Density Approximation (LDA) [50] is one of the simpler implementations of the density functional approach.

The Hartree-Fock approximation for the metal cluster electron structure has been originally worked out in the framework of spherically symmetric jellium model [51, 52]. It is valid for the clusters with closed electronic shells that correspond to magic numbers (8, 20, 34, 40,...). The open-shell two-center jellium Hartree-Fock approximation valid for metal clusters with arbitrary number of valence electrons has been developed recently [53–56]. The two-center jellium HF method treats the quantized electron motion in the field of the spheroidal ionic jellium background in the spheroidal coordinates. This method has been generalized and adapted to study of the metal clusters fission process in Refs. [13, 14].

The atomic system of units, $|e| = m_e = \hbar = 1$, is used throughout the paper, unless otherwise is indicated.

2. JELLIUM MODEL FOR CLUSTER FISSION

2.1. LIQUID DROP MODEL

The classical one center Liquid Drop Model (LDM) suggested by Lord Rayleigh in 1882 for fission of charged droplets [32] is a base of many approaches to the fission processes in nuclear [57] and in cluster physics [9, 34], where the uncompensated Coulomb forces deform a charged droplet which can

lead to fission. The Rayleigh model introduces the “fissility parameter”,

$$X = E_{Coul}^{sphere} / 2E_{Surf}^{sphere}, \quad (1)$$

which is defined as a ratio of the Coulomb to surface energy of charged liquid drop [32]. The competition between short-range attractive forces and long-range Coulomb repulsion forms the fission barrier, that separates the initial state from the fission products. For fissility $X \geq 1$ the droplet is unstable, spontaneously deforms and undergoes fission. The application of this result to metal clusters gives an estimate for the Rayleigh critical cluster size, N_{crit} , which depends on the surface tension and the Wigner-Seitz radius [1]. Indeed, the Coulomb and the surface energy of a charged spherical cluster with the excessive charge Z are expressed as

$$E_{Coul}^{sphere} = \frac{Z^2}{2R_0}, \quad (2)$$

$$E_{Surf}^{sphere} = 4\pi R_0^2 \sigma. \quad (3)$$

Here $R_0 = r_s N_0^{1/3}$ is the radius of the spherical cluster with the number of atoms N_0 , r_s is the Wigner-Seitz radius and σ is the surface tension. Therefore, the critical cluster size corresponding to $X = 1$,

$$N_{crit} = \frac{Z^2}{16\pi r_s^3 \sigma}. \quad (4)$$

This is the absolute lowest limit for stability [1]. For fissility $X = 1$ the droplet is unstable with respect to any small quadrupole deformations, while for values $X < 1$, fission from internally excited drops can be observed as long as the barrier remains comparable or smaller than the activation energy of evaporation of neutral particles [57].

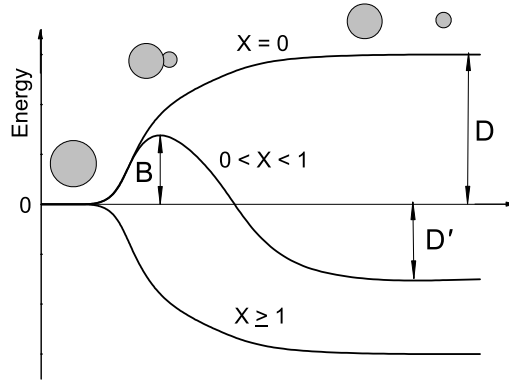


Fig. 1 – Fission barriers of charged liquid drops for different values of the fissility parameter X .

Schematically fission barriers of liquid drops are shown in Fig. 1. For large values of the fissility parameter $X \geq 1$, where the electrostatic energy dominates, fission is barrierless. For fissilities $X < 1$, the decay into two charged daughter fragments involves overcoming of a fission barrier, denoted B , due to an of the interplay between Coulomb repulsion and cohesive forces. The dissociation energy, $D' = E_{final} - E_{initial}$, is defined as a difference of the total energies of the final and the initial states of fissioning system. It can either be negative (decay is an exothermic process) or positive (decay is an endothermic process). Fissility $X = 0$ (i.e. $Z = 0$) corresponds to a neutral droplet. The neutral droplet is intrinsically stable and its decay is endothermic. In this case an excess of energy is necessary to promote decay. This can be achieved, e.g., by heating the droplet and making it thermally metastable. For neutral droplet, decay into two fragments is a barrierless process, and its rate is defined by the corresponding dissociation energy, D .

By careful examination of the fine structure in the mass spectra, it is possible to determine experimentally the critical size for appearance of multiply charged metal clusters [1, 18]. The experimental appearance size, N_{app}^{exp} , can be defined as the minimum size of the Z -fold charged clusters that can be identified in the spectrum.

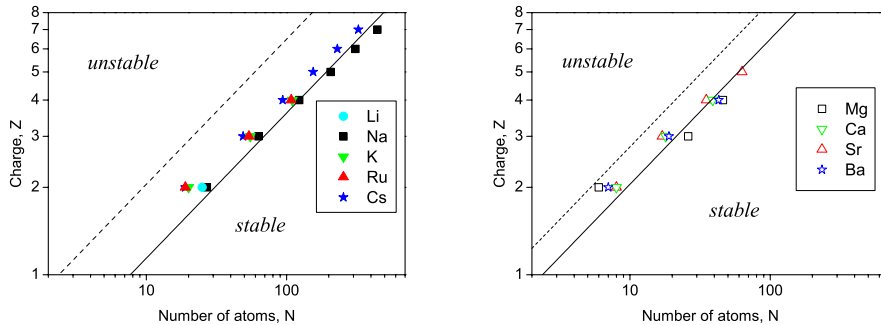


Fig. 2 – The experimentally observed appearance sizes, N_{app}^{exp} , of multiply charged alkali and alkaline earth metal clusters [1, 11]. The dashed lines correspond to the Rayleigh limit $X \approx 1$ ($Z^2/N = 0.4$ and 0.76 for the alkali and the alkaline earth metal clusters, respectively). The solid lines correspond to the observed appearance sizes of the alkali and the alkaline earth metal clusters, $X \approx 0.3$ ($Z^2/N = 0.13$) and $X \approx 0.55$ ($Z^2/N = 0.42$), respectively.

Figure 2 presents the values of N_{app}^{exp} determined from the mass spectra of hot alkali and alkaline earth metal clusters [1, 11, 18]. The experiments show that for alkali metal clusters fission begins to compete with evaporation at fissilities that lie in a narrow interval of X -values ($0.25 \leq X \leq 0.35$) and irrespective of which alkali metal one considers [1]. For alkaline earth metal

clusters the appearance sizes lie at the higher X-values ($0.50 \leq X \leq 0.73$) [11]. Thus, alkaline earth metal clusters are more stable against fission as compared with alkali metal clusters; their fissilities at appearance size being about twice as large as the values observed for the alkali metals [1, 11].

2.2. TWO-CENTER DEFORMED JELLIUM MODEL AND CLUSTER SHAPE PARAMETRIZATION

According to the main postulate of the jellium model, the electron motion in a metallic cluster takes place in the field of the uniform positive charge distribution of the ionic background. In Ref. [13] the two-center deformed jellium model for cluster fission was developed. In this model the initial parent cluster having the form of the spheroid splits into two independently deformed spheroids of smaller size [13]. The two principal diameters a_k and b_k of the spheroids can be expressed via the deformation parameter δ_k as

$$a_k = \left(\frac{2 + \delta_k}{2 - \delta_k} \right)^{2/3} R_k, \quad b_k = \left(\frac{2 - \delta_k}{2 + \delta_k} \right)^{1/3} R_k. \quad (5)$$

Here partial indexes $k = 0, 1, 2$ correspond to the parent cluster ($k = 0$) and the two daughter fragments ($k = 1, 2$), R_k ($k = 0, 1, 2$) are the radii of the corresponding undeformed spherical clusters. The deformation parameters δ_k characterize the families of the prolate ($\delta_k > 0$) and the oblate ($\delta_k < 0$) spheroids of equal volume $V_k = 4\pi a_k b_k^2/3 = 4\pi R_k^3/3$.

The radii of the parent and the resulting non overlapping daughter fragments are equal to $R_k = r_s N_k^{1/3}$, where N_k is the number of atoms in the k th cluster, and r_s is the Wigner-Seitz radius. For sodium clusters, $r_s = 4.0$, which corresponds to the density of the bulk sodium. For overlapping region the radii $R_1(d)$ and $R_2(d)$ are functions of the distance d between the centers of mass of the two fragments. They are determined in such a way that the total volume inside the two spheroids equals the volume of the parent cluster $4\pi R_0^3/3$.

The ions charge density $\rho(\mathbf{r})$ is kept uniform including the overlapping-spheroids region,

$$\rho(\mathbf{r}) = \begin{cases} \rho_c, & (x^2 + y^2)/b_1^2 + (z + d/2)^2/a_1^2 \leq 1 \\ \rho_c, & (x^2 + y^2)/b_2^2 + (z - d/2)^2/a_2^2 \leq 1 \\ 0, & \text{otherwise.} \end{cases} \quad (6)$$

Here $\rho_c = Z_0/V_0$ is the ionic charge density inside the cluster and Z_0 is the total charge of the ionic core.

The electrostatic potential $U_{core}(\mathbf{r})$ of the ionic background can be determined from the solution of the corresponding Poisson equation:

$$\Delta U_{core}(\mathbf{r}) = -4\pi\rho(\mathbf{r}). \quad (7)$$

2.3. NUMERICAL RESULTS

Let us discuss the results of calculations performed in the jellium models described above.

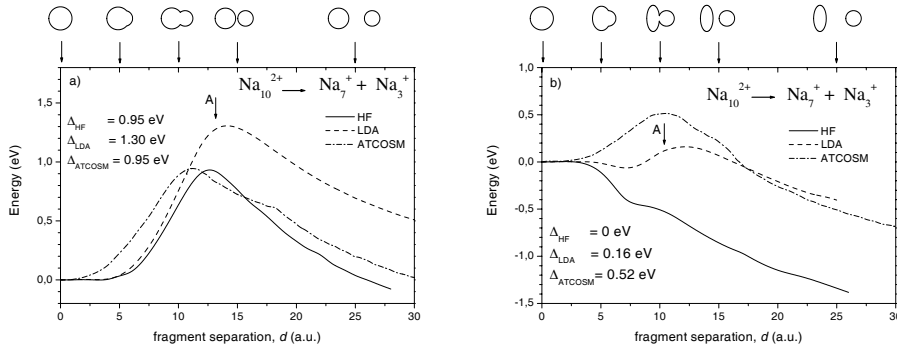


Fig. 3 – Fission barriers in the two-center deformed jellium Hartree-Fock (solid lines) and LDA (dashed lines) approaches [14] for the asymmetric channel $Na_{10}^{2+} \rightarrow Na_7^+ + Na_3^+$ as a function of fragments separation distance d . In (a), both parent and daughter clusters are spherical, $\delta_0 = \delta_1 = \delta_2 = 0$. In (b), deformations of the parent and daughter clusters are taken into account. The zero of energy put at $d = 0$. The evolution of cluster shape during the fission process is shown on top of figures (a) and (b) for both models. The HF and LDA results [14] are compared with those derived in ATCOSM [45] (dash-dotted line).

Figure 3 presents fission barriers for the asymmetric channel $Na_{10}^{2+} \rightarrow Na_7^+ + Na_3^+$ as a function of the fragments separation distance d . In order to perform the accurate comparison of fission barriers derived in the two-center deformed jellium HF and LDA models [14] with the ATCOSM results, [45] two different types of shape parametrization were used. Thus, the upper part in Fig. 3 shows the barriers for fission of a spherical parent cluster into two spherical daughter fragments (i.e. $\delta_0 = \delta_1 = \delta_2 = 0$). This type of parametrization, known as the two-intersected spheres parametrization, was used in many works [58, 59]. The low part in Fig. 3 shows fission barriers derived on the basis of parametrization accounting for an independent deformation of parent and daughter clusters in order to minimize the total energy of the system for any distance d . The evolution of cluster shape during the fission process

is shown for the HF and LDA models on tops of the corresponding figures. Note that the variable-necking-in parametrization was used in the ATCOSM calculation [45].

Solid lines in Fig. 3 are the result of the two-center jellium HF model, while dashed curves have been calculated in LDA (see Ref. [14]). Dash-dotted lines show the ATCOSM barriers calculated in Ref. [45]. The zero of energy put at $d = 0$.

Figure 3 (a) demonstrates a good agreement of the HF and ATCOSM fission barriers heights $\Delta_{HF} = \Delta_{ATCOSM} = 0.95$ eV. The LDA value for the fission barrier, $\Delta_{LDA} = 1.30$ eV, slightly exceeds the HF and ATCOSM ones. In the HF and LDA schemes the fission barrier maximum is located just behind the scission point (marked by vertical arrow A).

The two-intersected spheres parametrization is not adequate for the description of the process $Na_{10}^{2+} \rightarrow Na_7^+ + Na_3^+$, because Na_7^+ daughter fragment has an open-shell electronic structure, and therefore its shape is not spherical because it undergoes Jahn-Teller distortion [43]. The deformed jellium Hartree-Fock and LDA calculations show that the ground state of the Na_7^+ cluster has the oblate shape with the deformation parameter $\delta_1 = -0.68$. This value is in a good agreement with other theoretical estimates [53, 55]. The oblate shape deformation of the daughter cluster reduces the final total energy of the system E_{tot} by -1.32 eV for the HF, and by -1.05 eV for the LDA model calculations, in comparison with the spherical case.

Part (b), Fig. 3 shows fission barriers for the asymmetric channel $Na_{10}^{2+} \rightarrow Na_7^+ + Na_3^+$, when spheroidal deformations of the parent and daughter clusters are taken into account. The total energy of the system was minimized over the parent and daughter fragments deformations with the aim to find the fission pathway corresponding to the minimum fission barrier. The assumption of continuous shape deformation during the fission process was used in Ref. [14]. The deformation of the cluster fragments changes drastically the fission energetics in comparison with what follows from the two-intersected spheres model. In the framework of the two-center deformed jellium Hartree-Fock approximation, the parent cluster Na_{10}^{2+} becomes unstable [14] towards the asymmetric channel $Na_{10}^{2+} \rightarrow Na_7^+ + Na_3^+$.

The LDA simulations with deformation of the daughter fission fragments take into account the decrease of the total energy of the system (Fig. 3b). In particular, this results in appearance of the local minimum in the energy curve at $d = 7.2$ a.u., corresponding to the formation of the super deformed asymmetric prolate shape of the parent Na_{10}^{2+} cluster before the scission point A. The latter is located at $d = 10.4$ a.u. Deformation of the parent cluster and the fission fragments reduces the LDA fission barrier down to the value

$\Delta_{LDA} = 0.16$ eV, which is in a rather poor agreement with the result of ATCOSM $\Delta_{ATCOSM} = 0.52$ eV.

It is necessary to note that the shape of the cluster fragments in ATCOSM was parametrized [45] by two spheroids of revolution connected by a smooth neck along the axis z . Calculations performed in Ref. [14] show that the oblate shape of Na_7^+ fragment is formed at the initial stage of fission process, for separation distances before the scission point. Moreover, in the vicinity of the scission point, where the interaction between the two daughter fragments Na_7^+ and Na_3^+ is strong, the oblate Na_7^+ fragment is even more deformed than a free one. This means that it is more favourable for two fragments to split at shorter distances rather than to be connected by a smooth neck, making the system more prolate.⁴ This fact explains why using of necking type of shape parametrization within axially symmetric jellium model, leads to the higher barrier as compared to parametrization used in Ref. [14].

Comparison of the asymmetric $Na_{18}^{2+} \rightarrow Na_{15}^+ + Na_3^+$ and symmetric $Na_{18}^{2+} \rightarrow 2Na_9^+$ fission channels of the parent Na_{18}^{2+} cluster is a subject of particular interest, because a competition between these two channels involving magic cluster ions Na_3^+ and Na_9^+ is expected in this case. In Refs. [17, 23, 42] it was noticed that namely in fission of the Na_{18}^{2+} cluster a magic fragment other than Na_3^+ becomes the favoured channel. Figure 4 shows fission barriers for the asymmetric channel $Na_{18}^{2+} \rightarrow Na_{15}^+ + Na_3^+$. The initial configuration of the parent Na_{18}^{2+} cluster corresponds to oblate shape with the deformation parameter $\delta_0 = -0.35$ [13, 14]. The oblate deformation reduces the total energy of the cluster Na_{18}^{2+} by -0.58 eV for the HF and by -0.48 eV for the LDA model in comparison with the spherical case. In Ref. [14] the total energy of the system was minimized over the deformation parameters of the parent and daughter fragments during the fission process for any separation distance d . The evolution of the fragment shapes is shown on top of the figure for both HF and LDA models. The daughter fragment Na_{15}^+ has an oblate shape with deformation parameter $\delta_1 = -0.6$, while Na_3^+ is spherical, i.e. $\delta_2 = 0$.

The total energy as a function of the fragment separation distance has a maximum (marked by vertical arrow A for HF, and A' for LDA), arising due to the alteration of the electronic configuration $1\sigma^2 2\sigma^2 1\pi^4 2\pi^2 3\sigma^2 1\delta^4 \rightarrow 1\sigma^2 2\sigma^2 1\pi^4 3\sigma^2 4\sigma^2 1\delta^4$. These maxima on the energy curves define the fission barrier heights, being equal to $\Delta_{HF} = 0.36$ eV for Hartree-Fock and $\Delta_{LDA} = 0.50$ eV for LDA. It was noticed [14] that the LDA total energy curve has a pronounced minimum at $d = 12.5$ a.u., located beyond the scission point $d = 11.1$ a.u. The scission point is marked by vertical arrow B,

⁴ The results of molecular dynamics simulations demonstrate an importance of rearrangement of the cluster structure during fission [27]. It may include forming a neck between the two fragments or fissioning via another isomer state of the parent cluster.

both for HF and LDA. This minimum means that a quasistable state of the supermolecule $Na_{15}^+ + Na_3^+$ can be created during the fission process. However, the appearance of the minimum and thus the stability of the super molecule is rather sensitive to the model chosen for the description of exchange and correlation inter-electron interaction. This is already clear from the fact that such a minimum does not appear in the HF simulations (Fig. 4).

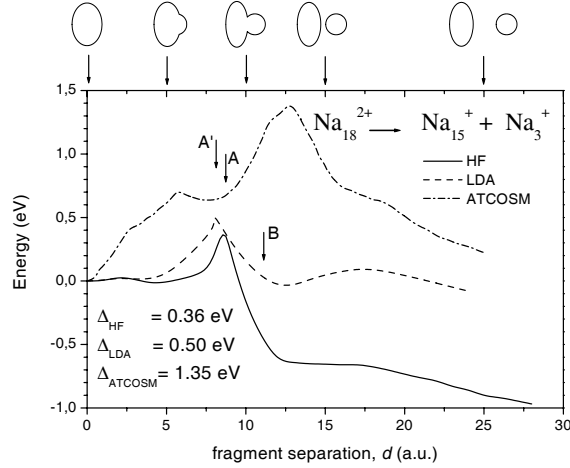


Fig. 4 – The same as Fig. 3, but for the asymmetric channel $Na_{18}^{2+} \rightarrow Na_{15}^+ + Na_3^+$.

The ATCOSM model calculation gives the value of the fission barrier $\Delta_{ATCOSM} = 1.35$ eV, which is inconsistent with the HF and LDA results. Such a difference can be explained as a result of variable-necking-in type of the shape parametrization, which has been used in Ref. [45]. In the case of asymmetric $Na_{18}^{2+} \rightarrow Na_{15}^+ + Na_3^+$ channel, the parent as well as one of the daughter fragments have an oblate shape, therefore shape parametrization model with prolate-like additional neck is not natural, and results in increasing the fission barrier.

Figure 5 shows the dependence of total energy E_{tot} on separation distance d for the symmetric channel $Na_{18}^{2+} \rightarrow 2Na_9^+$ calculated in Refs. [13, 14]. The parent cluster changes its shape from oblate to prolate one on the initial stage of the fission process ($d \approx 1$ a.u.). This transition is accompanied by the first re-arrangement of the electronic configuration (marked by vertical arrow A for HF and A' for LDA). This process has the barrier $\Delta_{HF} = 0.63$ eV and $\Delta_{LDA} = 0.48$ eV. On the next stage of the reaction the prolate deformation develops resulting in the highly deformed cluster shape, as it is shown on top of Fig. 5. At the distance $d \approx 11$ (marked by vertical arrow B for HF, and B' for LDA) the electronic configuration reaches its final form being the

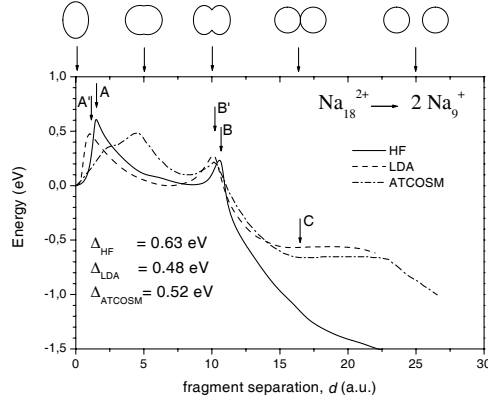


Fig. 5 – The same as Fig. 3, but for the symmetric channel $Na_{18}^{2+} \rightarrow 2Na_9^+$.

same as in the spherical Na_9^+ products. In this case, the variable-necking-in type of fragments shape parametrization used in ATCOSM does not break the symmetry of the fragments and therefore the agreement between the two overlapped spheroids HF or LDA models and ATCOSM variable-necking-in approach is much better than in the case of asymmetric fission channel. Indeed, the total fission barrier for the symmetric channel $Na_{18}^{2+} \rightarrow 2Na_9^+$ is equal to $\Delta_{HF} = 0.63$ eV and $\Delta_{LDA} = 0.48$ eV in the two-center jellium Hartree-Fock and LDA models, respectively. These values are in a good agreement with the ATCOSM result [45] $\Delta_{ATCOSM} = 0.52$ eV.

In Table 1 we have summarized the results of the HF, LDA (Refs. [13,14]) and ATCOSM (Ref. [45]) barrier heights calculations for the considered fission channels.

Table 1

Summary of the fission barrier heights in (eV) calculated in the HF, LDA and ATCOSM approximations

Channel	HF	LDA	ATCOSM [45]
$Na_{10}^{2+} \rightarrow Na_7^+ + Na_3^+$	0	0.16	0.52
$Na_{18}^{2+} \rightarrow Na_{15}^+ + Na_3^+$	0.36	0.50	1.35
$Na_{18}^{2+} \rightarrow 2Na_9^+$	0.63	0.48	0.52

3. SUMMARY

In summary, we have considered an open-shell two center jellium Hartree-Fock and LDA method for the description of the metal cluster fission process. The proposed two overlapping spheroids shape parametrization allows to consider independently wide variety of the shape deformations of the parent and

daughter clusters. The importance of deformation effects for the cluster fission process is demonstrated. Results obtained are in a good agreement with those described by ATCOSM method. Described model forms the basis for systematic development of the more advanced ab initio many-body theories for the process of atomic cluster fission.

Acknowledgements. This work is partially supported by the European Commission within the Network of Excellence project EXCELL, and by INTAS under the grant 03-51-6170. The authors gratefully acknowledge support by the Frankfurt Center for Scientific Computing.

REFERENCES

1. U. Näher, S. Bjornholm, F. Frauendorf, and C. Guet, *Phys. Rep.*, **285**, 245 (1997).
2. W. Ekardt (ed.), *Metal Clusters*, Wiley, New York, 1999.
3. C. Guet, P. Hobza, F. Spiegelman and F. David (eds.), *Atomic Clusters and Nanoparticles*, NATO Advanced Study Institute, les Houches Session LXXIII, les Houches, 2000, EDP Sciences and Springer Verlag, Berlin, 2001.
4. J.-P. Connerade and A.V. Solov'yov (ed.), *Latest Advances in Atomic Cluster Collisions: Fission, Fusion, Electron, Ion and Photon Impact*, Imperial College Press, London, 2004.
5. A. Lyalin, O.I. Obolensky, A.V. Solov'yov and W. Greiner, *Int. J. Mod. Phys., E* **15**, 153–195 (2006).
6. S.B. Nielsen, J.U. Andersen, P. Hvelplund, B. Liu, and S. Tomita, *J. Phys. B: At. Mol. Opt. Phys.*, **37**, R25 (2004).
7. R.S. Berry, A. Fernandez, and K. Kostov, *Eur. Phys. J., D* **16**, 47 (2001).
8. G. Gamov, *Z. Phys.*, **51**, 204 (1928).
9. K. Sattler, J. Mühlbach, O. Echt, P. Pfau, and, E. Recknagel *Phys. Rev. Lett.*, **47**, 160 (1981).
10. C. Bréchnignac, Ph. Cahuzac, F. Carlier, and M. de Frutos, *Phys. Rev. Lett.*, **64**, 2893 (1990).
11. M. Heinebrodt, S. Frank, N. Malinowski, F. Tast, I.M.L. Billas, and T.P. Martin, *Z. Phys., D* **40**, 334 (1997).
12. C. Yannouleas, U. Landman, and R.N. Barnett, in *Metal Clusters*, edited by W. Ekardt, Wiley, New York, 1999, p. 145.
13. A.G. Lyalin, S.K. Semenov, A.V. Solov'yov, and W. Greiner, *Phys. Rev., A* **65**, 023201 (2002).
14. A. Lyalin, A. Solov'yov and W. Greiner, *Phys. Rev., A* **65**, 043202 (2002).
15. T.P. Martin, *J. Chem. Phys.*, **81**, 4426 (1984).
16. C. Bréchnignac, Ph. Cahuzac, F. Carlier, and J. Leygnier, *Phys. Rev. Lett.*, **63**, 1368 (1989).
17. C. Bréchnignac, Ph. Cahuzac, F. Carlier, J. Leygnier, and A. Sarfati, *Phys. Rev., B* **44**, 11386 (1991).
18. T.P. Martin, U. Nähler, H. Göhlich, and T. Lange, *Chem. Phys. Lett.*, **196**, 113 (1992).
19. C. Bréchnignac, Ph. Cahuzac, F. Carlier, and M. de Frutos, *Phys. Rev., B* **49**, 2825 (1994).

20. S. Kruckeberg, L. Schweikhard, G. Dietrich, K. Lutzenkirchen, C. Walther, J. Ziegler, *Chemical Physics*, **262**, 105 (2000).
21. C. Yannouleas, U. Landman, C. Bréchnignac, Ph. Cahuzac, B. Concina, and J. Leygnier, *Phys. Rev. Lett.*, **89**, 173403 (2002).
22. O. I. Obolensky, A.G. Lyalin, A.V. Solov'yov, and W. Greiner, *Phys. Rev.*, B **72**, 085433 (2005).
23. R.N. Barnett, U. Landman, and G. Rajagopal, *Phys. Rev. Lett.*, **67**, 3058 (1991); P. Jena, S.N. Khanna, and C. Yannouleas, *Phys. Rev. Lett.*, **69**, 1471 (1992).
24. R.N. Barnett, U. Landman, A. Nitzan, and G. Rajagopal, *J. Chem. Phys.*, **94**, 608 (1991).
25. C. Guet, X. Biquard, P. Blaise, S.A. Blundell, M. Gross, B.A. Huber, D. Jalabert, M. Maurel, L. Plagne, and J.C. Rocco, *Z. Phys.*, D **40**, 317 (1997).
26. F. Calvayrac, P.-G. Reinhard and E. Suraud, *J. Phys. B: At. Mol. Opt. Phys.*, **31**, 5023 (1998).
27. A.G. Lyalin, O.I. Obolensky, A.V. Solov'yov, Il.A. Solov'yov, and W. Greiner, *J. Phys. B: At. Mol. Opt. Phys.*, **37**, L7 (2004).
28. A. Lyalin, O. Obolensky, Il. Solov'yov, A. Solov'yov and W. Greiner, *Physica Scripta*, **T110**, 319 (2004).
29. A. Lyalin, O. Obolensky, Il.A. Solov'yov, A.V. Solov'yov, and W. Greiner, in *Latest Advances in Atomic Cluster Collisions: Fission, Fusion, Electron, Ion and Photon Impact*, edited by J.-P. Connerade and A.V. Solov'yov, Imperial College Press, London, 2004, p. 157.
30. A. Lyalin, A.V. Solov'yov, C. Bréchnignac, and W. Greiner, *J. Phys. B: At. Mol. Opt. Phys.*, **38**, L129 (2005).
31. A. Lyalin, O.I. Obolensky, A.V. Solov'yov, and W. Greiner, *Eur. Phys. J.*, D **34**, 93 (2005).
32. Lord Rayleigh, *Philos. Mag.*, **14**, 185 (1882).
33. W.A. Saunders, *Phys. Rev. Lett.*, **64**, 3046 (1990).
34. W.A. Saunders, *Phys. Rev.*, A **46**, 7028 (1992).
35. F. Chandezon, S. Tomita, D. Cormier, P. Grübling, C. Guet, H. Lebius, A. Pesnelle, and B.A. Huber, *Phys. Rev. Lett.*, **87**, 153402 (2001).
36. J.M. Eisenberg, and W. Greiner, *Nuclear Theory*, Vol. 1, "Collective and Particle Models", North Holland, Amsterdam, 1985.
37. V.M. Strutinsky, *Nucl. Phys.*, A **95**, 420 (1967).
38. V.M. Strutinsky, *Nucl. Phys.*, A **122**, 1 (1968).
39. C. Yannouleas, and U. Landman, *Chem. Phys. Lett.*, **210**, 437 (1993).
40. S.M. Reimann, M. Brack, and K. Hansen, *Z. Phys. D: At., Mol. Clusters*, **28**, 235 (1993).
41. H. Koizumi, S. Sugano, and Y. Ishii, *Z. Phys.*, D **28**, 223 (1993).
42. C. Yannouleas and U. Landman, *Phys. Rev.*, B **51**, 1902 (1995).
43. S. Frauendorf and V.V. Pashkevich, *Ann. Phys. (Leipzig)*, **5**, 34 (1996).
44. J. Maruhn and W. Greiner, *Z. Phys.*, **251**, 431 (1972).
45. C. Yannouleas and U. Landman, *J. Phys. Chem.*, **99**, 14577 (1995).
46. W. Ekardt, W.D. Schöne, and J.M. Pacheco, in *Metal Clusters*, edited by W. Ekardt, Wiley, New York, 1999, p. 1.
47. R.G. Parr and W. Yang, *Density-Functional Theory of Atoms and Molecules*, Oxford University Press, Oxford, New York, 1989.
48. P. Fulde, *Electron Correlations in Molecules and Solids*, Springer-Verlag, Berlin, 1995.
49. D. Salahub, in Ref. [3].
50. W. Kohn and L.J. Sham, *Phys. Rev.*, A **140**, 1133 (1965).

51. C. Guet and W.R. Johnson, *Phys. Rev.*, B **45**, 11283 (1992).
52. V.K. Ivanov, A.N. Ipatov, V.A. Kharchenko, and M.L. Zhizhin, *Phys. Rev.*, A **50**, 1459 (1994).
53. A.G. Lyalin, S.K. Semenov, A.V. Solov'yov, N.A. Cherepkov, and W. Greiner, *J. Phys. B: At. Mol. Opt. Phys.*, **33**, 3653 (2000)
54. A.G. Lyalin, S.K. Semenov, A.V. Solov'yov, N.A. Cherepkov, J.-P. Connerade, and W. Greiner, *J. Chin. Chem. Soc. (Taipei)*, **48**, 419 (2001).
55. A. Matveentzev, A.G. Lyalin, I.I. Solov'yov, A.V. Solov'yov, and W. Greiner, *Int. Journal of Mod. Phys., E* **12**, 81 (2003).
56. A.G. Lyalin, A. Matveentzev, I.I. Solov'yov, A.V. Solov'yov, and W. Greiner, *Eur. Phys. Journal, D* **24**, 15, (2003).
57. N. Bohr and J.A. Wheeler *Phys. Rev.*, **56**, 426 (1939).
58. S. Saito and M.L. Cohen, *Phys. Rev.*, B **38**, 1123 (1988).
59. E. Engel, U.R. Schmitt, H.-J. Lüdde, A. Toepfer, E. Wüst, R.M. Dreizler, O. Knospe, R. Schmidt, and P. Chattopadhyay *Phys. Rev.*, B **48**, 1862 (1993).